General Pathway toward Crystalline-Core Micelles with Tunable Morphology and Corona Segregation

Joachim Schmelz,[†] Matthias Karg,[‡] Thomas Hellweg,[§] and Holger Schmalz[†,*]

[†]Makromolekulare Chemie II, Universität Bayreuth, 95440 Bayreuth, Germany, [‡]Physikalische Chemie I, Universität Bayreuth, 95440 Bayreuth, Germany, and [§]Physikalische und Biophysikalische Chemie, Universität Bielefeld, 33615 Bielefeld, Germany

ABSTRACT

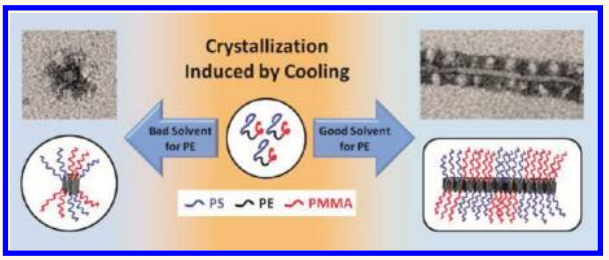

We present a general mechanism for the solution self-assembly of crystalline-core micelles (CCMs) from triblock copolymers bearing a semicrystalline polyethylene (PE) middle block. This approach enables the production of nanoparticles with tunable dimensions and surface structures. Depending on the quality of the solvent used for PE, either spherical or worm-like CCMs can be generated in an easy and highly selective fashion from the same triblock copolymers *via* crystallization-induced self-assembly upon cooling. If the triblock copolymer stays molecularly dissolved at temperatures above the crystallization temperature of the PE block, worm-like CCMs with high aspect ratios are formed by a nucleation and growth process. Their length can be conveniently controlled by varying the applied crystallization temperature. If exclusively spherical micelles with an amorphous PE core are present before crystallization, confined crystallization within the cores of the preformed micelles takes place and spherical CCMs are formed. For polystyrene-*block*-polyethylene-*block*-poly(methyl methacrylate) triblock terpolymers a patch-like microphase separation of the corona is obtained for both spherical and worm-like CCMs due to the incompatibility of the PS and PMMA blocks. The structure of the patch-like corona depends on the selectivity of the employed solvent for the PS and PMMA corona blocks, whereby nonselective solvents produce a more homogeneous patch size and distribution. Annealing of the semicrystalline PE cores results in an increasingly uniform crystallite size distribution and thus core thickness of the worm-like CCMs.

KEYWORDS: nanostructures · crystalline-coil block copolymers · cylindrical micelles · patchy particles · surface compartmentalization

Due to their fascinating properties, block copolymers have been investigated intensively during the past decades. In solid state as well as in solution, their self-assembly allows the production of a variety of unique structures with promising applications in, for example, materials science, biomedicine, and optoelectronics.[1−3] However, the majority of research in the field, especially regarding structure formation in solution, is focused on coil−coil block copolymers.[4] Even though early theoretical work predicted the formation of spherical (or "hockey-puck"), cylindrical, and lamellar (platelet-like) structures by solution self-assembly of crystalline-coil block copolymers,[5] only recently has significant effort in exploiting their unique properties been undertaken.[6−8] For these systems, solution self-assembly is controlled by the crystallization of one polymer block, which is triggered by the addition of a nonsolvent or cooling below its crystallization temperature. Here, especially the ability to produce stable cylindrical or worm-like micelles of high aspect ratio is of rising interest in materials science and biotechnology.[6,9] Among the still rather few systems used in this field, block copolymers with a polyferrocenylsilane (PFS) block have been studied most extensively, allowing the production of cylindrical, tubular, and sheet-like structures with a crystalline PFS core surrounded by various types of amorphous corona blocks.[10−12] Manners and Winnik *et al.* showed that the cylindrical micelles are formed *via* crystallization-driven living self-assembly, which enables the precise control of the cylinder length and length distribution using seeded crystallization with small seed micelles formed by sonication or self-seeding.[7,13,14] This living self-assembly was used to produce more complex architectures, also, *e.g.*, block-*co*-micelles, scarf-like micelles, as well as brush layers grown from PFS homopolymer surfaces.[7,8] Other examples of one-dimensional structures formed upon crystallization include polybutadiene-*block*-poly(ethylene oxide),[15] poly(ε-caprolactone)-*block*-poly(ethylene oxide) with poly(ε-caprolactone) as the crystallizing block,[16,17] poly(3-hexylthiophene)-*block*-poly(dimethylsiloxane),[18] polyacrylonitrile-based block copolymers,[19,20]

* Address correspondence to holger.schmalz@uni-bayreuth.de.

Received for review July 14, 2011 and accepted November 2, 2011.

Published online November 02, 2011
10.1021/nn202638t

© 2011 American Chemical Society

and enantiopure polylactide-containing diblock copolymers.[21,22]

With regard to the polyethylene (PE)-containing systems studied up to now, mostly platelet- or disk-like aggregates have been observed.[23−25] To the best of our knowledge, only in our recent work about a polystyrene-*block*-polyethylene-*block*-poly(methyl methacrylate) triblock terpolymer could one-dimensional structures be formed from a linear PE-containing block copolymer.[26] Interestingly, for PE-*b*-PEP (PEP: poly(ethylene-*alt*-propylene)) diblock copolymer stars with PE inner blocks cylindrical micelles were found, whereas platelets were formed again when the outer blocks of the stars consist of PE.[27] In this case, unimolecular hockey-puck micelles with rare events of intermolecular cocrystallization were assumed to form a pearl-necklace structure, loosely connected by amorphous segments. Similar mechanisms comprising the aggregation of initially formed spherical crystalline-core micelles to one- or two-dimensional assemblies have also been discussed for block copolymers with poly(ethylene oxide) and poly(ε-caprolactone) as crystallizable blocks.[28−30] In contrast, for PFS-containing cylindrical micelles, a partial nucleation followed by the deposition of remaining unimers to these seeds was reported.[6,7] However, understanding the processes of block copolymer crystallization in solution is still at an early stage, and hence, further knowledge of the parameters that control this promising type of self-assembly is needed to make predictions with respect to the formed structures.

Another highly active research field, in which block copolymer self-assembly plays a decisive role, is the production of surface-compartmentalized nanostructures. Nanoparticles with defined surface anisotropies show interesting properties and offer a wide range of applications, *e.g.*, outstanding surface activity, the formation of hierarchically ordered superstructures, and the potential use as scaffolds for the directed incorporation of metallic nanoparticles.[31−33] The simplest form of surface compartmentalization, two separated compartments (or faces) of different chemistry and/or polarity, can be found in Janus particles, where spherical, cylindrical, and disk-like architectures have been produced.[31,34−36] Recently, the synthesis of patchy particles, consisting of more than two different compartments, came into the focus of several research groups.[32,37−41] However, mostly spherical patchy micelles have been produced so far. One-dimensional structures with distinct corona compartments have hardly been observed, even though theoretical work predicts their existence.[42] A P*t*BA-*b*-PCEMA-*b*-PGMA (poly(*tert*-butyl acrylate)-*block*-poly(2-cinnamoyloxyethyl methacrylate)-*block*-poly(glyceryl monomethacrylate)) triblock terpolymer has been used to form a variety of structures such as cylinders, vesicles, and tubes in selective solvents for the end blocks.[43] Here, the P*t*BA blocks form small circular patches in a corona mainly consisting of PGMA. From a similar P*t*BA-*b*-PCEMA-*b*-PBMA (PBMA = poly(*n*-butyl methacrylate)) triblock terpolymer even double and triple helices could be produced *via* hierarchical self-assembly of patch-like cylindrical micelles triggered by the addition of a nonsolvent for one of the corona blocks.[44] In general, the production of surface-compartmentalized nanostructures is challenging and usually requires arduous, time-consuming sample preparation including dialysis into solvent mixtures, cross-linking, and/or template-assisted approaches.[31,34,35,37,38,43]

Recently, we reported the formation of worm-like micelles from a polystyrene-*block*-polyethylene-*block*-poly(methyl methacrylate) triblock terpolymer (PS-*b*-PE-*b*-PMMA) by crystallization-induced self-assembly from solution.[26] These worm-like micelles exhibit a patchy corona of PS and PMMA, thus integrating the feature of surface compartmentalization into a system with high aspect ratio. The advantage of this process over existing ones is the comparatively undemanding and time-efficient production of surface-compartmentalized one-dimensional nanostructures by simply cooling a polymer solution in order to trigger crystallization and hence self-assembly. However, the mechanism of structure formation still remains an unresolved issue. In this publication we provide a thorough investigation of the fundamental parameters influencing this self-assembly process. From the obtained results we propose a general mechanism for the self-assembly of triblock copolymers with semicrystalline middle blocks from solution. This allows control not only of the morphology of the formed crystalline-core micelles (CCMs), *i.e.*, spherical *vs* worm-like, by a careful selection of the solvent environment, but also of the extent of surface compartmentalization, *i.e.*, patchy *vs* homogeneous corona. Furthermore, we will show that the self-assembly of PS-*b*-PE-*b*-PMMA triblock terpolymers with identical block lengths of the PS and PMMA end blocks in THF gives access to worm-like CCMs with a unique highly regular one-dimensional array structure of equally sized alternating PS and PMMA corona patches.

RESULTS AND DISCUSSION

In a previous work we studied the self-assembly of a polystyrene-*block*-polyethylene-*block*-poly(methyl methacrylate) triblock terpolymer in organic solvents (toluene and THF) and found exclusively worm-like crystalline-core micelles (wCCMs) with a patch-like corona.[26] However, the mechanism of one-dimensional growth and the influence of variables such as concentration, crystallization temperature, polymer composition, overall molecular weight, and solvent quality were not addressed.

In this publication we now identify the key parameters for the formation of CCMs in order to tune their

morphology as well as the microphase separation in the corona. First, the structure formation process of polystyrene-*block*-polyethylene-*block*-poly(methyl methacrylate) triblock terpolymers ($S_xE_yM_z$: subscripts denote the number-average degree of polymerization) in toluene and THF (good solvents for molten polyethylene; see Table S1) will be studied. This includes variations in crystallization temperature and polymer concentration, polyethylene content, and overall molecular weight of the $S_xE_yM_z$ triblock terpolymers. In addition, a polystyrene-*block*-polyethylene-*block*-polystyrene triblock copolymer ($S_{380}E_{880}S_{390}$) is examined, in order to identify whether the incompatibility of the polystyrene (PS) and poly(methyl methacrylate) (PMMA) corona blocks influences the formed morphology. Subsequently, the solvent quality for PE is decreased using dioxane and *N*,*N*-dimethylacetamide as solvents for the self-assembly. From the obtained results we deduce a general mechanism for the selective formation of wCCMs or sCCMs (spherical crystalline-core micelles) from the same triblock copolymers.

The used $S_xE_yM_z$ triblock terpolymers and the $S_{380}E_{880}S_{390}$ were prepared *via* catalytic hydrogenation of the corresponding $S_xB_yM_z$ and $S_{380}B_{440}S_{390}$ (B = poly(1,4-butadiene)) triblock copolymer precursors, which were synthesized by sequential anionic polymerization. Details on the synthesis can be found in the Methods section.

Structure Formation in Good Solvents for PE. To gain a deeper insight into the mechanism of the crystallization process in solution, first the crystallization temperature was varied. Thus, isothermal crystallization was conducted at different temperatures for 2 g/L toluene solutions of $S_{340}E_{700}M_{360}$ (detailed information about the used triblock copolymers can be found in Table S2), which we followed in real time by static light scattering (Figure 1).

For these crystallization experiments, all polymer solutions were preheated to 80 °C to ensure complete melting of the PE blocks. After cooling to the desired crystallization temperature with a cooling rate of about 2 K/min, the scattering intensity I_S was monitored as a function of time. For all applied temperatures I_S increases with time until a plateau is reached. This increase can be attributed to the crystallization-induced structure formation process.

In addition, a clear tendency is observed for all crystallization temperatures. Faster structure formation occurs for lower crystallization temperatures; that is, a shorter time span is needed until the scattering intensity reaches its final plateau value, indicating complete structure formation (Table 1). Furthermore, the final scattering intensity that is reached after complete structure formation decreases with decreasing crystallization temperature. This points to a decrease in the length of the formed wCCMs, since this goes along with a decrease in the radius of gyration as well as in aggregation number and thus molecular weight. However, it has to be noted that the intensity of the scattered light for worm-like objects depends on additional parameters such as the particle form factor, and, hence, only qualitative trends are extracted from the light scattering data presented in Figure 1.

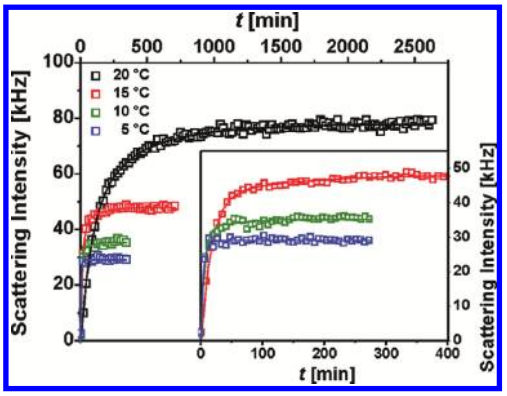

Figure 1. Intensity of scattered light *vs* time for 2 g/L toluene solutions of $S_{340}E_{700}M_{360}$ cooled to different crystallization temperatures as indicated. The inset shows a close-up of the data obtained at lower crystallization temperatures.

TABLE 1. Characteristics of wCCMs Formed by Isothermal Crystallization of 2 g/L Toluene Solutions of $S_{340}E_{700}M_{360}$ at Different Temperatures

T_{cryst} [°C][a]	l_{wCCMs} [nm][b]	t_{SF} [min][c]	$I_{S,\infty}$ [kHz][d]
20	520 (260)	1600	78
15	330 (170)	240	48
10	280 (160)	140	36
5	240 (140)	50	29

[a] Applied isothermal crystallization temperature. [b] Average micelle length derived from TEM image analysis of at least 100 micelles (standard deviation in parentheses). [c] Time of structure formation, defined as the time when the scattering intensity no longer deviates more than 5% from the final scattering intensity. [d] The final scattering intensity $I_{S,\infty}$ corresponds to the mean scattering intensity of the last two hours of the experiment.

To verify the assumptions drawn from light scattering, the formed wCCMs were investigated by transmission electron microscopy (TEM). For all TEM images shown in this article PS was selectively stained by RuO_4 vapor prior to investigation, resulting in dark PS domains. PMMA domains and the PE core appear bright, as they are not affected by this staining procedure.[26] Figure 2 shows two representative TEM micrographs of wCCMs prepared by isothermal crystallization at 20 and 5 °C, respectively. In both images wCCMs with a PE core (bright) surrounded by a microphase-separated corona of PS (dark) and PMMA (bright) can be observed. For a crystallization temperature of 20 °C wCCMs with lengths up to about 1 μm are obtained, whereas those crystallized at 5 °C are significantly shorter on average, as revealed by image analysis.

The results summarized in Table 1 strongly support the previous assumption that the observed drop in the final scattering intensity $I_{S,\infty}$ corresponds to a decrease

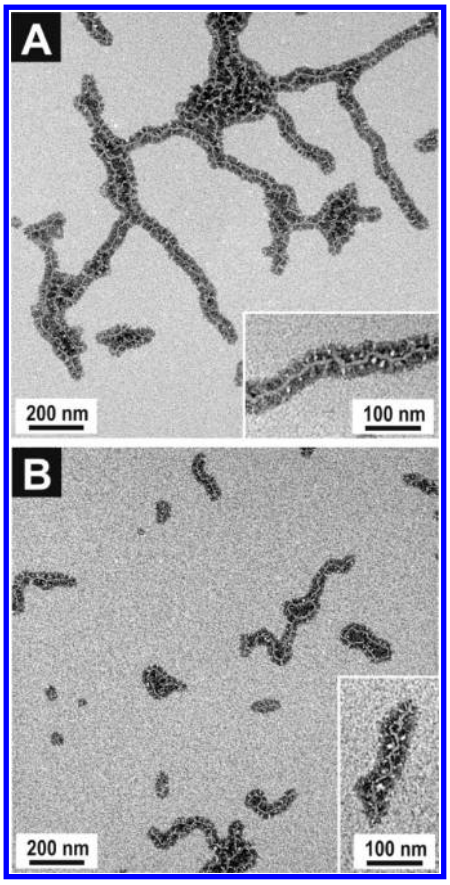

Figure 2. Worm-like CCMs obtained from 2 g/L toluene solutions of $S_{340}E_{700}M_{360}$ by isothermal crystallization at (A) 20 °C and (B) 5 °C. The solutions were diluted to 0.25 g/L before drop-coating onto carbon-coated copper grids.

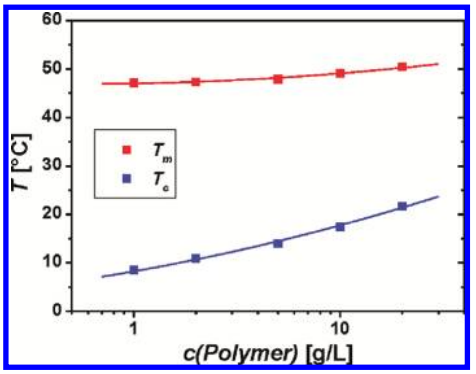

Figure 3. Peak melting (T_m) and crystallization (T_c) temperatures *vs* polymer concentration as derived from μDSC measurements on $S_{340}E_{700}M_{360}$ solutions in toluene. Lines are drawn to guide the eyes.

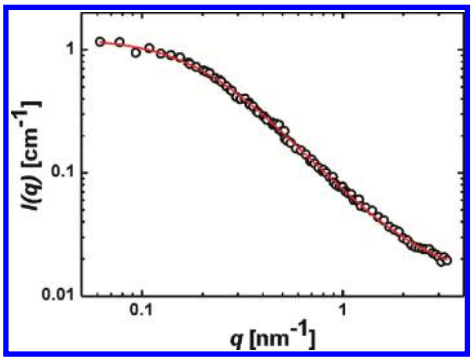

Figure 4. SANS profile of $S_{340}E_{700}M_{360}$ measured at 70 °C in toluene-d_8 (10 g/L). The solid line is a fit with a model for Gaussian polymer coils including a Gaussian polydispersity.

of the average micelle length l_{wCCMs}. Moreover, the observed decrease in wCCM length upon lowering the crystallization temperature points to a nucleation and growth process. For equally concentrated solutions with respect to the crystallizable polymer the probability of forming stable nuclei is expected to increase at higher supercooling, similar to the behavior for crystallization from the melt.[45] As a result, the limited amount of dissolved polymer chains has to be distributed among more nuclei, and consequently shorter wCCMs are obtained at lower temperatures. Hence, variation of the crystallization temperature provides a convenient method to tune the average micelle length.

In a nucleation and growth process the concentration of crystallizable polymer should also have an influence on the crystallization. Accordingly, we investigated the concentration dependency of the crystallization process using microdifferential scanning calorimetry (μDSC) of differently concentrated $S_{340}E_{700}M_{360}$ solutions in toluene (Figure 3).

The range of concentrations (1−20 g/L; for μDSC heating and cooling traces see Figure S1) was chosen for practical reasons, as for concentrations ≥ 30 g/L a gel is formed upon cooling due to entanglement of the long wCCMs, which might have an impact on the crystallization process. For concentrations below 1 g/L on the other hand, the enthalpy changes of melting/crystallization are very low and, thus, reach the detection limit of the μDSC apparatus. Lowering the concentration, we observe a significant decrease in the peak crystallization temperature (T_c) from 21.7 °C for 20 g/L to 8.5 °C for 1 g/L, respectively. This again supports a nucleation and growth process. The probability of creating stable nuclei from a semicrystalline polymer in solution decreases with concentration, as is predicted by theory[46,47] and was already shown for crystallization of PE homopolymers from solution.[48] As a result, higher supercoolings are required for crystallization at low concentrations. The melting endotherms, in contrast, show only a very small shift to higher peak melting temperatures (T_m) upon increasing concentration (from 47.2 to 50.4 °C). It has to be noted that both melting and crystallization occur at significantly lower temperatures compared to the same triblock terpolymer in bulk (T_c = 62 °C; T_m = 88 °C).[26] This can be attributed to toluene acting as a plasticizer for the semicrystalline PE block, taking into account that toluene is a good solvent for PE in the molten state (Table S1).[49]

In order to fully understand this nucleation and growth mechanism, knowledge about the initial state, *i.e.*, the triblock terpolymer solution at temperatures

well above the melting temperature of the PE block, is essential, also. Therefore, we conducted small-angle neutron scattering (SANS) on a $S_{340}E_{700}M_{360}$ solution at 70 °C in toluene-d_8 (Figure 4).

The resulting scattering intensity trace could be fitted with a model for Gaussian polymer coils providing a radius of gyration of 8 ± 2 nm, showing that the majority of the triblock terpolymer is molecularly dissolved. The SANS profile does not show a significant contribution of micellar aggregates, which would give rise to an upturn of $I(q)$ at low q-values. This is in agreement with previous results from DLS and scanning force microscopy that suggested a solution consisting of molecularly dissolved unimers and a negligible fraction of micellar aggregates.[26] It is noted that DLS strongly overestimates the contribution of aggregates present in solution as the scattering intensity scales with R^6 in the case of spherical micelles. The polymer–solvent interaction parameter $\chi_{PE-toluene}$ = 0.39 (Table S1) also supports a good solubility of PE above its melting temperature. Combining the obtained information, the formation of wCCMs from $S_{340}E_{700}M_{360}$ in toluene can be described as a nucleation and growth process originating from a unimer solution.

For semicrystalline bulk polymers, annealing of existing crystallites can be used to perfect the crystallite structure, resulting in less folds and hence an increased crystallite thickness accompanied by a more uniform crystallite thickness distribution.[50] In order to see whether also in the present case an improvement of the preformed wCCMs can be achieved by subsequent solution-annealing of the PE cores, we performed μDSC annealing experiments on a 10 g/L toluene solution of $S_{340}E_{700}M_{360}$. A detailed description of the applied annealing procedure and the corresponding μDSC traces can be found in the Supporting Information (Scheme S1, Figure S2). These measurements revealed that most effective annealing takes place at 45 °C. The nonannealed wCCMs exhibit a rather broad melting peak ranging from 35 to 55 °C. In contrast, the heating trace after annealing the solution of the wCCMs at 45 °C for 3 h shows two distinct melting peaks (Figure 5): an intense, sharp one at a higher peak temperature compared to the initial melting endotherm (50.4 °C compared to 48.9 °C), and a very small one at lower temperatures corresponding to the fraction of unimers that were not able to participate in the annealing process and thus crystallized upon subsequent cooling. The increased melting temperature of the main peak corresponds to an increase in crystallite thickness, as can be described by the Gibbs–Thomson equation.[51] In addition, the melting peak becomes significantly narrower after annealing, which indicates a more uniform crystallite thickness distribution. Annealing of samples with lower concentrations (1 g/L) shows similar effects

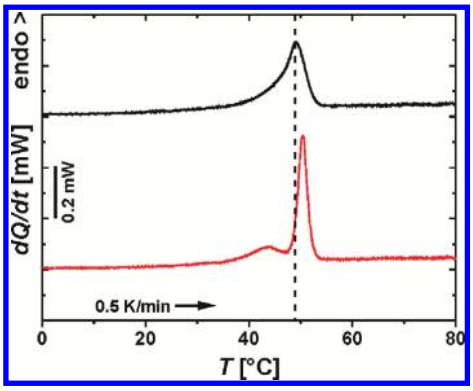

Figure 5. μDSC heating traces of a 10 g/L toluene solution of $S_{340}E_{700}M_{360}$ wCCMs before (black line) and after (red line) annealing for 3 h at 45 °C. The dashed line indicates the peak melting temperature before annealing.

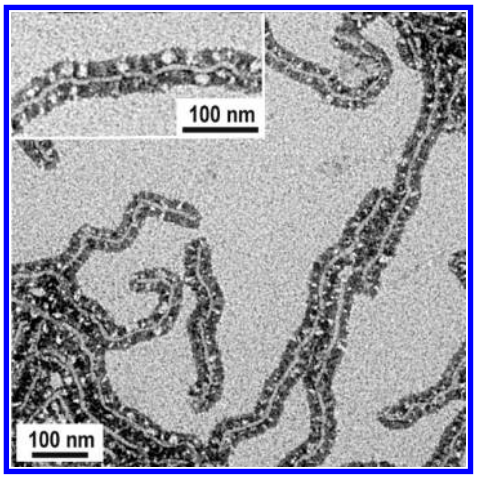

Figure 6. TEM micrograph of wCCMs formed in a 1 g/L solution of $S_{340}E_{700}M_{360}$ in toluene, crystallized at 20 °C, and subsequently annealed for 3 h at 45 °C.

(Figure S3) and is hereinafter applied as standard treatment prior to morphological studies by TEM.

The TEM image of $S_{340}E_{700}M_{360}$ wCCMs (Figure 6), which have been crystallized at 20 °C and subsequently annealed at 45 °C for 3 h, confirms a more uniform overall morphology and thickness of the PE cores compared to the nonannealed sample (Figure 2A). Moreover, the microphase separation between PS and PMMA in the micellar corona is somewhat more pronounced, which can be explained by the melting of some of the PE crystallites in the core, allowing a partial rearrangement of the corona blocks during the annealing process. A similar observation of increasing microphase separation upon annealing was reported for amphiphilic block terpolymers in water.[52]

A solvent of comparable quality to toluene is THF. The polymer–solvent interaction parameter, χ_{PE-THF} = 0.41, is very similar to that for toluene ($\chi_{PE-toluene}$ = 0.39), and therefore, also THF should be able to dissolve PE in the molten state, *i.e.*, at elevated temperatures. μDSC measurements show that the transition temperatures and the annealing behavior of $S_{340}E_{700}M_{360}$ in THF are

very similar to those in toluene (Figure S4, Table S3). Due to the low boiling point of THF, $S_{340}E_{700}M_{360}$ was dissolved at 65 °C for 30 min, which is still significantly higher than the melting temperature of the PE block (T_m = 52.0 °C), followed by isothermal crystallization at 20 °C for one day and annealing at 45 °C for 3 h. As expected, TEM images again show wCCMs with a patch-like microphase separation of the corona (Figure 7).

In contrast to the structures obtained from toluene, in which the diameter of the PMMA patches was rather small (D = 7 ± 4 nm), nonuniform, and mostly randomly distributed throughout the corona, significantly larger PMMA patches (D = 13 ± 4 nm) are observed for the wCCMs formed in THF. These PMMA patches exhibit a more defined shape spanning out from the PE core to the outer rim of the corona. In many sections, a regular one-dimensional array of alternating PS and PMMA corona patches is obtained (Figure 7). The observed differences should emanate from the selectivity of the used solvent for PS and PMMA. Toluene is known to be a better solvent for PS than for PMMA, whereas THF is supposed to be an equally good solvent for both corona blocks.[53] Thus, in toluene the PMMA chains are less swollen compared to PS and therefore form smaller compartments in an almost continuous PS corona despite the similar block lengths. In THF both of the corona blocks exhibit good solubility, favoring the formation of compartments of almost equal size.

Impact of the Triblock Copolymer Composition. In order to gain further understanding of the parameters favoring one-dimensional micellar growth, we synthesized two additional triblock terpolymers, $S_{280}E_{1190}M_{300}$ and $S_{140}E_{690}M_{160}$, both of them possessing a higher weight content of PE. Therefore, structures with a lower curvature, *i.e.*, lamellae (platelet-like), might be energetically favored for these copolymers, as was predicted in early theoretical works[5] and already observed several times experimentally.[24,54] Moreover, the overall molecular weight of $S_{140}E_{690}M_{160}$ is by a factor of about 2 lower compared to that of $S_{280}E_{1190}M_{300}$ and the previously used polymer. A decrease in overall molecular weight is also expected to promote platelet formation, as was shown by Ryan *et al.*[30] However, in our case, wCCMs with a microphase-separated corona are obtained for both $S_{280}E_{1190}M_{300}$ and $S_{140}E_{690}M_{160}$ (Figure 8A,B), showing that the formation of linear structures is applicable to a wide range of block terpolymer compositions. As revealed by μDSC experiments (Figure S5, Table S3), the crystallization is shifted to higher temperatures, because of the increased PE content. Thus, crystallization was conducted at 29 °C for $S_{140}E_{690}M_{160}$ and 34 °C for $S_{280}E_{1190}M_{300}$ followed by annealing at 38 and 48 °C for 3 h, respectively.

Another possible influence on the structure formation process might emanate from the incompatibility of the PS and PMMA corona blocks, which results in a less effective shielding of the PE core of the formed

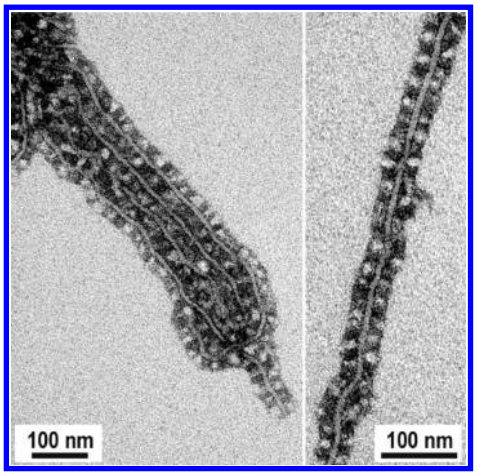

Figure 7. TEM micrographs of wCCMs formed in a 1 g/L $S_{340}E_{700}M_{360}$ solution in THF after annealing at 45 °C for 3 h.

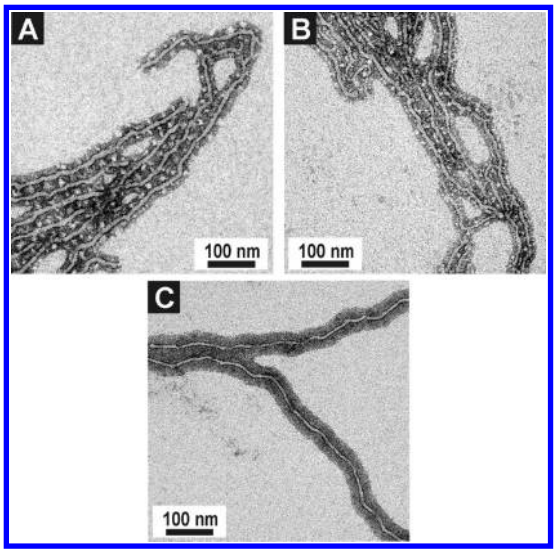

Figure 8. TEM images of wCCMs formed in 1 g/L THF solutions of $S_{280}E_{1190}M_{300}$ (A), $S_{140}E_{690}M_{160}$ (B), and $S_{380}E_{880}S_{390}$ (C), annealed in solution.

nuclei by the corona. This in turn would favor one-dimensional growth over the formation of spherical micelles, as already assumed earlier.

Consequently, a different situation might be expected for a triblock copolymer with identical end blocks. In order to address this point, a $S_{380}E_{880}S_{390}$ triblock copolymer, comparable in block ratios and overall degree of polymerization to $S_{340}E_{700}M_{360}$, was synthesized. μDSC experiments revealed similar thermal properties compared to that of $S_{340}E_{700}M_{360}$ (Table S3), and thus $S_{380}E_{880}S_{390}$ was crystallized at 20 °C followed by annealing at 45 °C for 3 h, *i.e.*, the same protocol as applied for $S_{340}E_{700}M_{360}$. However, despite the identical PS end blocks, $S_{380}E_{880}S_{390}$ forms wCCMs in THF, also (Figure 8C). In this case the corona appears homogeneously dark after staining, as expected for a corona that solely consists of PS. The self-assembly of $S_{380}E_{880}S_{390}$ clearly shows that the

formation of one-dimensional, elongated micelles does not depend on repulsive forces generated by PS/PMMA segregation in the corona, but seems to be independent of the chemical nature of the outer blocks.

The fact that wCCMs have been obtained from various $S_xE_yM_z$ triblock terpolymers as well as the $S_{380}E_{880}S_{390}$ triblock copolymer leads to the assumption that the middle position of the PE block is the key factor triggering one-dimensional growth over a broad composition range. This theory is corroborated by literature, as only one of the various studied systems with distinct PE blocks was found capable of cylinder formation upon crystallization, *i.e.*, PE-*b*-PEP diblock copolymer stars with PE in the center of the stars.[27] Here, PE is in the middle position surrounded by amorphous end blocks, in analogy to the triblock copolymers investigated in this study.

Structure Formation in Bad Solvents for PE. Up to this point, structure formation was conducted in good solvents for PE ($\chi_{PE-solvent} < 0.5$). We now focus on the self-assembly in dioxane, which is a good solvent for the corona blocks, but a poor solvent for PE ($\chi_{PE-dioxane} = 0.75$). μDSC measurements (Figure 9A) reveal transition temperatures of 79 °C (peak melting) and 44 °C (peak crystallization) for a 1 g/L solution of $S_{340}E_{700}M_{360}$. These temperatures are significantly higher compared to those observed in toluene (Figure 3, Table S3), which can be attributed to the lower solvent quality of dioxane for PE. Consequently, dioxane is not a good plasticizer and thus is not able to decrease melting and crystallization temperatures to a similar extent. In contrast to toluene solutions, no concentration dependency of the crystallization temperature (Figure S6) is observed for dioxane solutions.

The structure formation upon cooling was followed by dynamic light scattering (DLS) on a 1 g/L solution of $S_{340}E_{700}M_{360}$ in dioxane. First, the solution was heated to 85 °C for 2 h, *i.e.*, above the melting temperature of the PE block, and subsequently cooled to 70 °C and then to room temperature. Figure 9B shows the corresponding hydrodynamic radii distributions obtained at different temperatures applying the CONTIN algorithm.[55] At 85 °C the absolute scattering intensity is very low and a broad distribution with an average apparent hydrodynamic radius of $R_{h,app} = 9$ nm can be found, which corresponds to molecularly dissolved triblock terpolymer chains. Already at 70 °C, a narrow distribution at $R_{h,app} = 24$ nm is observed, pointing to the formation of well-defined micelles. As mentioned above, dioxane is a rather poor solvent for PE. Thus, PE becomes insoluble upon cooling to 70 °C, and spherical micelles with an amorphous PE core are formed, as the temperature is still significantly above the crystallization temperature (T_c = 44 °C). The weak peak at about 76 °C in the μDSC cooling trace (Figure 9A) also corresponds to this micellization

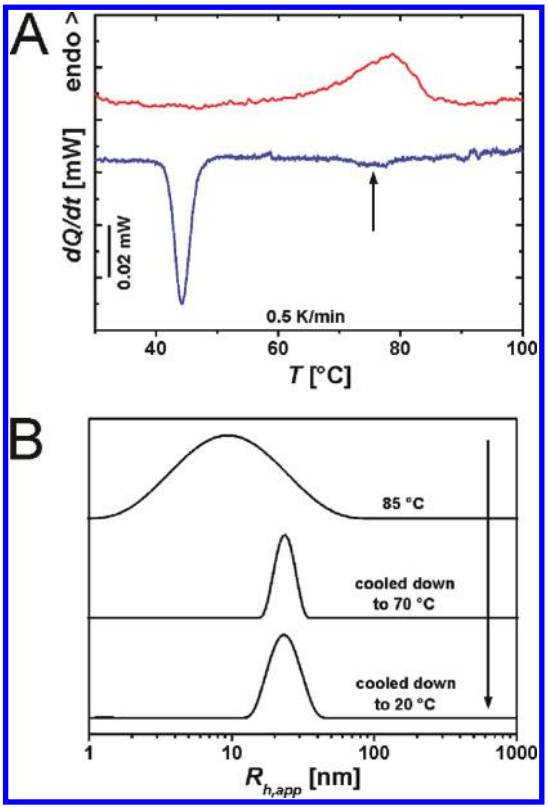

Figure 9. (A) μDSC heating (red) and cooling traces (blue) of a 1 g/L dioxane solution of $S_{340}E_{700}M_{360}$. The arrow highlights the weak micellization peak. (B) Apparent hydrodynamic radii distributions obtained from DLS data measured for a 1 g/L dioxane solution of $S_{340}E_{700}M_{360}$ at temperatures as indicated.

process. It is exothermic in nature, as should be expected for micellization in organic solvents. The weak exotherm, attributable to the micellization process upon cooling, is present for all studied $S_{340}E_{700}M_{360}$ and $S_{380}E_{880}S_{390}$ solutions in dioxane (Figure S6) and has also been observed for similar block copolymers in dioxane.[56] Upon cooling the solution to room temperature, $R_{h,app}$ does not change. Hence, the overall shape and size of the micelles are preserved, and PE undergoes confined crystallization within the micellar core, resulting in spherical crystalline-core micelles (sCCMs). Similar examples of confined crystallization were reported for block copolymers in the bulk state, where the crystallizable block is confined within spherical microdomains.[57] In a PE-*b*-PS diblock copolymer, homogeneous nucleation was assumed for the crystallization of PE in spherical microdomains. Here, a supercooling $\Delta T = T_m - T_c$ of about 39 °C was necessary to induce crystallization.[58] In our case, the supercooling observed for $S_{340}E_{700}M_{360}$ in dioxane (ΔT = 35 °C) and the confinement in which crystallization occurs, *i.e.*, the core of spherical micelles, are comparable. Moreover, the degree of crystallinity of the PE cores in the sCCMs formed in dioxane is significantly lower compared to that of the wCCMs formed in toluene or THF (Table S3), which is a typical feature of

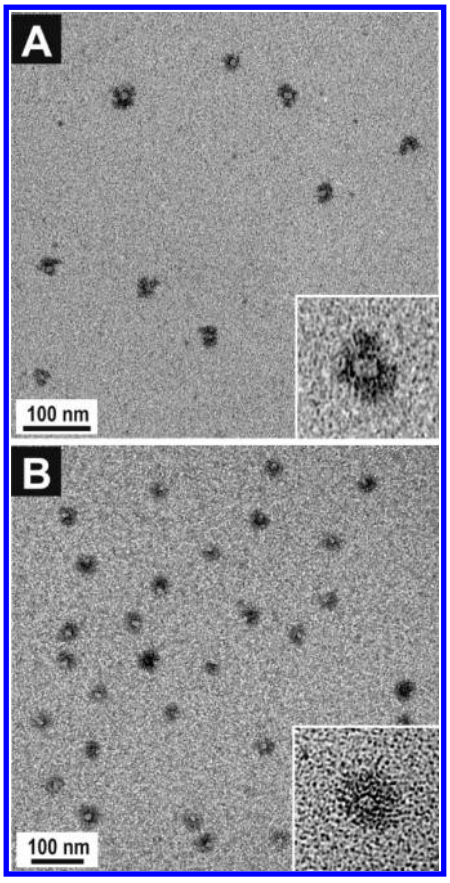

Figure 10. TEM micrographs of sCCMs formed in 1 g/L dioxane solutions of $S_{340}E_{700}M_{360}$ (A) and $S_{380}E_{880}S_{390}$ (B). The solutions were kept for three weeks at room temperature prior to sample preparation for TEM. (A) was diluted to 0.3 g/L before drop-coating on the TEM grid. The insets are magnified 3-fold.

confined crystallization. Consequently, a homogeneous nucleation should be the predominant nucleation mechanism for PE in the sCCMs. Structure formation of $S_{380}E_{880}S_{390}$ in dioxane proceeds in a similar way. μDSC and DLS results for $S_{380}E_{880}S_{390}$ in dioxane can be found in Figures S6 and S7.

TEM investigations confirm the formation of sCCMs for both types of triblock copolymers (Figure 10). The sCCMs formed from $S_{340}E_{700}M_{360}$ exhibit a microphase-separated corona of stained PS patches (dark) and nonstained PMMA patches (bright). Those composed of $S_{380}E_{880}S_{390}$ consequently show a uniformly dark corona of PS.

Whereas the sCCMs made of $S_{380}E_{880}S_{390}$ could be nicely dispersed on the TEM grid from a 1 g/L solution, for those consisting of $S_{340}E_{700}M_{360}$ further dilution to 0.3 g/L was necessary to reduce the aggregation to superstructures during drying (Figure S8). The formation of such superstructures is a known feature of surface-compartmentalized polymer micelles and thus supports the patch-like structure of the corona for sCCMs based on $S_xE_yM_z$ triblock terpolymers.[59] It is noted that the TEM samples were prepared after

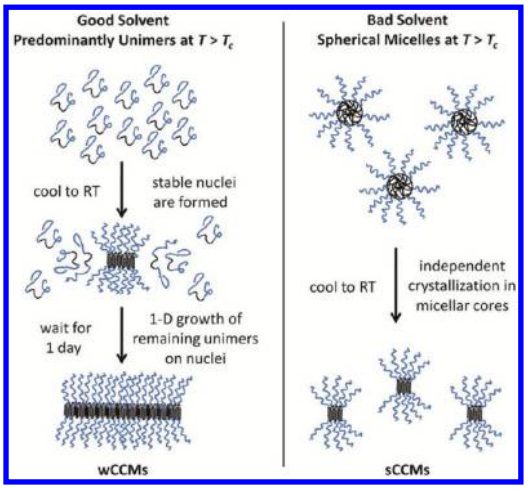

Scheme 1. Proposed mechanism of the structure formation of triblock copolymers with a crystallizable PE middle block (black) and amorphous corona blocks (blue) in solvents of different quality.

keeping the solution at room temperature for three weeks, showing that these sCCMs are stable over time and do not form worm-like structures *via* aggregation/recrystallization processes.

In order to prove the general applicability of this concept, structure formation of $S_{340}E_{700}M_{360}$ in *N*,*N*-dimethylacetamide (DMAc) was conducted, which is an even worse solvent for PE than dioxane ($\chi_{PE-DMAc}$ = 1.18). The solution was heated to 100 °C overnight to erase any thermal history of PE and subsequently allowed to cool to room temperature. In analogy to the structure formation in dioxane, sCCMs with a microphase-separated corona are obtained (Figure S9). Hence, the self-assembly in poor solvents for PE can be utilized as a general method for the production of sCCMs and is attributed to the collapse of PE upon cooling, producing amorphous spherical micelles already above T_c.

Mechanism of Structure Formation. From the observed differences in the structure formation of the studied triblock copolymers with PE middle blocks a general scheme can be deduced that determines whether spherical or worm-like CCMs are formed (Scheme 1). The comparison of $S_xE_yM_z$ and $S_{380}E_{880}S_{390}$ revealed that the nature of the outer blocks is not important for the overall morphology, as long as they are sufficiently soluble in the chosen solvent throughout the applied temperature range. Thus, for the sake of clarity, we did not distinguish between the possibilities of different or equal outer blocks in this case.

The essential parameter determining the morphology, wCCMs *vs* sCCMs, is the solubility of the molten PE in the applied solvent. The use of good solvents such as toluene and THF, where PE is completely soluble at $T > T_c$, enables the production of wCCMs with high aspect ratios. Upon lowering the temperature, at some point first nucleation events occur, producing a small

number of micelles with a crystalline PE core. Over time, more and more unimers are deposited onto these crystalline micelles, resulting in the observed wCCMs. In poor solvents on the other hand, *e.g.*, dioxane and DMAc, sCCMs are formed. Here, PE is insoluble at $T > T_c$, and thus, spherical micelles with a molten PE core already exist prior to crystallization. The PE cores of the spherical micelles then crystallize independently upon cooling, as the sterically demanding corona chains prevent micellar fusion, an effect known as "overspilling".[60] Thus, the availability of free unimers at the stage where crystallization occurs is identified as the key factor for the formation of anisotropic worm-like micelles from triblock terpolymers with a PE middle block. These findings allow the highly selective production of sCCMs and wCCMs from the same block copolymers by carefully choosing the solvent environment for the crystallization-induced structure formation.

CONCLUSIONS

We introduce a general scheme predicting the crystallization-induced self-assembly of triblock copolymers with a semicrystalline PE middle block upon cooling in solution. Depending on the solubility of PE in the used solvent, the selective production of either spherical or worm-like crystalline-core micelles from the same block copolymers is possible. These CCMs consist of a semicrystalline PE core and a uniform (PS-*b*-PE-*b*-PS triblock copolymer) or a patchy (PS-*b*-PE-*b*-PMMA triblock terpolymer) corona. Spherical CCMs are formed in poor solvents for molten PE; that is, the PE blocks collapse upon cooling and spherical micelles with amorphous cores are formed prior to crystallization. As a result, confined crystallization of PE within the cores of the preformed spherical micelles takes place. In contrast, the triblock copolymer chains stay molecularly dissolved above the crystallization temperature for self-assembly in good solvents, and worm-like CCMs are formed *via* a nucleation and growth mechanism.

The length of the worm-like CCMs can be conveniently tuned by the applied temperature of isothermal crystallization. Further improvement of their structure is achieved by subsequent annealing in solution. This results in a more uniform thickness of the crystalline PE cores, and the corona microphase separation in wCCMs based on PS-*b*-PE-*b*-PMMA triblock terpolymers becomes more pronounced. Furthermore, the morphology of the patch-like corona depends on the selectivity of the used solvent for the PS and PMMA end blocks. In toluene, a slightly better solvent for PS, small PMMA patches in an almost continuous corona of PS are obtained. In contrast, structure formation in THF, a similarly good solvent for PS and PMMA, results in a unique one-dimensional array structure with nearly alternating PS and PMMA patches with dimensions of about 15 nm throughout the whole corona.

The presented approach enables the selective production of stable worm-like micelles with high aspect ratios and controlled surface anisotropies in an easy and reproducible manner, which is of increasing interest in materials science. Linear array structures represent promising scaffolds for waveguides in nanoscale photonic devices. Moreover, well-defined patchy nanoparticles have great potential for the tailor-made bottom-up production of hierarchical superstructures. In contrast to most of the previous approaches toward surface-compartmentalized nanostructures, the presented process of crystallization-driven solution self-assembly triggered by cooling is comparably undemanding and easy to scale up.

METHODS

Synthesis of Triblock Copolymers. Detailed information about used materials, purification methods, and the polymerization procedure applied for the synthesis of polystyrene-*block*-poly(1,4-butadiene)-*block*-poly(methyl methacrylate) triblock terpolymers can be found in a previous publication.[61]

The synthesis of polystyrene-*block*-poly(1,4-butadiene)-*block*-polystyrene (PS-*b*-PB-*b*-PS) was carried out in a thermostated laboratory autoclave (Büchi Glas Uster AG) under a dry nitrogen atmosphere *via* sequential anionic polymerization of the corresponding monomers in cyclohexane. The use of a nonpolar solvent results in a PB block with a high content of 1,4-addition, which is indispensable to obtain the corresponding semicrystalline "pseudo-polyethylene" structure after hydrogenation. First, styrene was polymerized at 40 °C for 4 h using *sec*-BuLi as the initiator. The reaction mixture was then cooled to 20 °C, and butadiene was added. Subsequently, butadiene polymerization was conducted at 50 °C for 4 h. Finally, the second portion of styrene was allowed to polymerize for 4 h at 40 °C followed by termination with methanol. The composition of the produced triblock copolymer $S_{380}B_{440}S_{390}$ (the subscripts denote the number-average degree of polymerization) was determined by ^{1}H NMR measurements in $CDCl_3$ (Bruker AC 250 spectrometer) using the absolute molecular weight of the PS precursor, obtained from matrix-assisted laser desorption ionization time-of-flight mass spectrometry (MALDI-TOF; Bruker Reflex III), for calibration of the NMR signal intensities.

Hydrogenation. Hydrogenation of the triblock copolymers in order to convert the PB block into PE was carried out *via* homogeneous catalysis in toluene at 60 °C and 60 bar H_2 pressure using Wilkinson's catalyst ($RhCl(PPh_3)_3$). A more detailed description can be found elsewhere.[26]

Sample Preparation. The triblock copolymers were dissolved at temperatures well above the melting temperature of the PE block in the used solvents to erase any thermal history. The samples prepared in toluene and THF were heated in a water bath to 70 and 65 °C, respectively, for at least 30 min after complete dissolution, followed by direct quenching to the desired crystallization temperature. Except for the studies on the influence of the applied crystallization temperature, all solutions of worm-like CCMs prepared for TEM measurements were subjected to subsequent annealing for 3 h at a temperature slightly below the melting temperature, as indicated in the Results and Discussion section. The samples prepared in dioxane were heated to 90 °C, and those prepared in *N*,*N*-dimethylacetamide to 100 °C overnight and subsequently allowed to

cool to room temperature. In all cases moderate stirring was applied.

Micro-Differential Scanning Calorimetry. The calorimetric measurements were performed with a Setaram μDSC III using closed "batch" cells at a scanning rate of 0.5 K/min. The pure solvent was used as a reference. The μDSC allows measurements with an extremely high sensitivity using sample masses up to 1 g and hence the detection of phase transitions of polymers in dilute solutions.

Dynamic Light Scattering and Static Light Scattering. DLS and SLS measurements were performed on an ALV DLS/SLS-SP 5022F compact goniometer system equipped with an ALV 5000/E operated in cross-correlation mode at a scattering angle of 90°. A He−Ne laser (λ_0 = 632.8 nm) was employed as light source.

Because of the large size of the aggregates formed at room temperature, the solutions were not filtered prior to the measurement to avoid any loss of material. The decalin bath of the instrument was thermostated using a LAUDA Proline RP 845 thermostat. For the temperature steps, heating rates of about 3 K/min and cooling rates of about 2 K/min were applied. Prior to measurement, the solutions were allowed to equilibrate for at least 10 min after reaching the targeted temperature, except for the time-dependent SLS measurements, where data collection was started directly after reaching the desired crystallization temperature. The structure formation studies by SLS were conducted at a scattering angle of 90°, which represents a value of momentum transfer $q = 0.014$ nm^{-1}. This value of q is more than 1 order of magnitude lower than the expected first form factor minimum of the wCCMs (q_{min}). On the basis of the diameter of $S_{340}E_{700}M_{360}$ wCCMs determined from TEM (D = 51 nm) a form factor minimum at $q_{min} = 0.25$ nm^{-1} can be calculated. Hence, the performed SLS measurements are in a q-range much lower than the Guinier region, and form factor contributions to the scattering intensity can be neglected. However, a quantitative interpretation of the scattering intensity is difficult and not in the scope of the present contribution. The results from SLS are used only to show a qualitative trend.

Data evaluation of the DLS experiments was performed using the CONTIN algorithm,[55] which yields an intensity-weighted distribution of relaxation times (τ) after an inverse Laplace transformation of the intensity autocorrelation function. These relaxation times were transformed into translational diffusion coefficients and further into hydrodynamic radii using the Stokes−Einstein equation.

Transmission Electron Microscopy. Samples were prepared by placing a drop of the dilute solution (0.25−1 g/L) on a carbon-coated copper grid. After 20 s, excess solution was removed by blotting with a filter paper. Subsequently, elastic bright-field TEM was performed on a Zeiss 922 OMEGA EFTEM (Zeiss NTS GmbH, Oberkochen, Germany) operated at 200 kV. Zero-loss filtered images (ΔE = 0) were registered digitally by a bottom-mounted CCD camera system (Ultrascan 1000, Gatan) and processed with a digital imaging processing system (Gatan Digital Micrograph 3.9 for GMS 1.4). Staining was performed with RuO_4 vapor for at least 20 min. RuO_4 is known to selectively stain PS; that is, PS domains appear darker compared to PMMA domains, which enables distinguishing between PS and PMMA domains in the corona of the micelles. Average values of the micelle length and PMMA patch size were determined from at least 100 measurements. Due to better visibility, the average micelle length of the wCCMs was obtained by measuring the core length.

Small-Angle Neutron Scattering. The SANS measurement was performed on the PAXY instrument of the Laboratoire Léon Brillouin (CEA de Saclay, Gif-sur-Yvette, France). The scattered neutrons were collected using a two-dimensional multidetector. Three sample-to-detector distances of 1.05 m, 3.05 m, and 6.75 m were chosen in order to cover a sufficiently broad q-range. The sample was placed in a thermostated holder, and the temperature was controlled using a PT 100 thermoelement with stability in temperature of approximately ±1 °C. The sample was prepared in deuterated toluene (C_7D_8) and filled in 1 mm standard quartz cells (Hellma, Germany).

All recorded scattering patterns were isotropic and hence circularly averaged. Furthermore, the resulting spectra were corrected for electronic noise, detector efficiency, and the scattering of the empty cell and the solvent. The absolute intensity calibration was done using the software provided by the LLB using the approach described by Cotton.[62] Further information on the data treatment procedure of the LLB can be found elsewhere.[63] After this treatment all data from different sample-to-detector distances overlapped within the experimental precision. Finally, the normalized and merged scattering profile was analyzed applying the SASfit program by J. Kohlbrecher.[64]

Acknowledgment. This work was supported by the German Science Foundation in the framework of the Collaborative Research Center SFB 840 (project A2). We acknowledge the allocation of SANS beamtime at the Laboratoire Léon Brillouin (Saclay, France) and assistance during the SANS experiments by A. Lapp. J.S. appreciates support from the Elite Network of Bavaria and the University of Bavaria. M.K. thanks the Alexander von Humboldt foundation for a Feodor Lynen fellowship. We acknowledge helpful discussions with G. Reiter (Albert-Ludwig-University of Freiburg).

Supporting Information Available: Molecular characteristics of the used triblock copolymers, additional μDSC results on $S_xE_yM_z$ triblock terpolymers in toluene, polymer−solvent interaction parameters, and further details on the structure formation of $S_{340}E_{700}M_{360}$ and $S_{380}E_{880}S_{390}$ in dioxane, as well as $S_{340}E_{700}M_{360}$ in DMAc. This material is available free of charge *via* the Internet at http://pubs.acs.org.

REFERENCES AND NOTES

1. Haberkorn, N.; Lechmann, M. C.; Sohn, B. H.; Char, K.; Gutmann, J. S.; Theato, P. Templated Organic and Hybrid Materials for Optoelectronic Applications. *Macromol. Rapid Commun.* **2009**, *30*, 1146–1166.
2. Motornov, M.; Roiter, Y.; Tokarev, I.; Minko, S. Stimuli-Responsive Nanoparticles, Nanogels and Capsules for Integrated Multifunctional Intelligent Systems. *Prog. Polym. Sci.* **2010**, *35*, 174–211.
3. Ruzette, A. V.; Leibler, L. Block Copolymers in Tomorrow's Plastics. *Nat. Mater.* **2005**, *4*, 19–31.
4. Rodríguez-Hernández, J.; Chécot, F.; Gnanou, Y.; Lecommandoux, S. Toward 'Smart' Nano-Objects by Self-Assembly of Block Copolymers in Solution. *Prog. Polym. Sci.* **2005**, *30*, 691–724.
5. Vilgis, T.; Halperin, A. Aggregation of Coil-Crystalline Block Copolymers: Equilibrium Crystallization. *Macromolecules* **1991**, *24*, 2090–2095.
6. Lazzari, M.; Lopez-Quintela, M. A. Micellization Phenomena in Semicrystalline Block Copolymers: Reflexive and Critical Views on the Formation of Cylindrical Micelles. *Macromol. Rapid Commun.* **2009**, *30*, 1785–1791.
7. Wang, X.; Guerin, G.; Wang, H.; Wang, Y.; Manners, I.; Winnik, M. A. Cylindrical Block Copolymer Micelles and Co-Micelles of Controlled Length and Architecture. *Science* **2007**, *317*, 644–647.
8. Gaedt, T.; Ieong, N. S.; Cambridge, G.; Winnik, M. A.; Manners, I. Complex and Hierarchical Micelle Architectures from Diblock Copolymers Using Living, Crystallization-Driven Polymerizations. *Nat. Mater.* **2009**, *8*, 144–150.
9. Qian, J. S.; Zhang, M.; Manners, I.; Winnik, M. A. Nanofiber Micelles from the Self-Assembly of Block Copolymers. *Trends Biotechnol.* **2010**, *28*, 84–92.
10. Raez, J.; Barjovanu, R.; Massey, J. A.; Winnik, M. A.; Manners, I. Self-Assembled Organometallic Block Copolymer Nanotubes. *Angew. Chem., Int. Ed.* **2000**, *39*, 3862–3865.
11. Raez, J.; Tomba, J. P.; Manners, I.; Winnik, M. A. A Reversible Tube-to-Rod Transition in a Block Copolymer Micelle. *J. Am. Chem. Soc.* **2003**, *125*, 9546–9547.
12. Cao, L.; Manners, I.; Winnik, M. A. Influence of the Interplay of Crystallization and Chain Stretching on Micellar Morphologies: Solution Self-Assembly of Coil-Crystalline Poly(isoprene-*block*-ferrocenylsilane). *Macromolecules* **2002**, *35*, 8258–8260.

13. Gilroy, J. B.; Gaedt, T.; Whittell, G. R.; Chabanne, L.; Mitchels, J. M.; Richardson, R. M.; Winnik, M. A.; Manners, I. Monodisperse Cylindrical Micelles by Crystallization-Driven Living Self-Assembly. *Nat. Chem.* **2010**, *2*, 566–570.
14. Qian, J.; Guerin, G.; Lu, Y.; Cambridge, G.; Manners, I.; Winnik, M. A. Self-Seeding in One Dimension: An Approach to Control the Length of Fiberlike Polyisoprene–Polyferrocenylsilane Block Copolymer Micelles. *Angew. Chem., Int. Ed.* **2011**, *50*, 1622–1625.
15. Mihut, A. M.; Drechsler, M.; Möller, M.; Ballauff, M. Sphere-to-Rod Transition of Micelles Formed by the Semicrystalline Polybutadiene-*block*-poly(ethylene oxide) Block Copolymer in a Selective Solvent. *Macromol. Rapid Commun.* **2010**, *31*, 449–453.
16. Du, Z.-X.; Xu, J.-T.; Fan, Z.-Q. Regulation of Micellar Morphology of PCL-*b*-PEO Copolymers by Crystallization Temperature. *Macromol. Rapid Commun.* **2008**, *29*, 467–471.
17. He, W. N.; Xu, J. T.; Du, B. Y.; Fan, Z. Q.; Wang, X. S. Inorganic-Salt-Induced Morphological Transformation of Semicrystalline Micelles of PCL-*b*-PEO Block Copolymer in Aqueous Solution. *Macromol. Chem. Phys.* **2010**, *211*, 1909–1916.
18. Patra, S. K.; Ahmed, R.; Whittell, G. R.; Lunn, D. J.; Dunphy, E. L.; Winnik, M. A.; Manners, I. Cylindrical Micelles of Controlled Length with a π-Conjugated Polythiophene Core via Crystallization-Driven Self-Assembly. *J. Am. Chem. Soc.* **2011**, *133*, 8842–8845.
19. Lazzari, M.; Scalarone, D.; Hoppe, C. E.; Vazquez-Vazquez, C.; Lopez-Quintela, M. A. Tunable Polyacrylonitrile-Based Micellar Aggregates as a Potential Tool for the Fabrication of Carbon Nanofibers. *Chem. Mater.* **2007**, *19*, 5818–5820.
20. Lazzari, M.; Scalarone, D.; Vazquez-Vazquez, C.; Lopez-Quintela, M. A. Cylindrical Micelles from the Self-Assembly of Polyacrylonitrile-Based Diblock Copolymers in Nonpolar Selective Solvents. *Macromol. Rapid Commun.* **2008**, *29*, 352–357.
21. Portinha, D.; Boué, F.; Bouteiller, L.; Carrot, G.; Chassenieux, C.; Pensec, S.; Reiter, G. Stable Dispersions of Highly Anisotropic Nanoparticles Formed by Cocrystallization of Enantiomeric Diblock Copolymers. *Macromolecules* **2007**, *40*, 4037–4042.
22. Petzetakis, N.; Dove, A. P.; O'Reilly, R. K. Cylindrical Micelles from the Living Crystallization-Driven Self-Assembly of Polylactide-containing Block Copolymers. *Chem. Sci.* **2011**, *2*, 955–960.
23. Monkenbusch, M.; Schneiders, D.; Richter, D.; Willner, L.; Leube, W.; Fetters, L. J.; Huang, J. S.; Lin, M. Aggregation Behaviour of PE-PEP Copolymers and the Winterization of Diesel Fuel. *Phys. B (Amsterdam, Neth.)* **2000**, *276–278*, 941–943.
24. Wang, J.; Horton, J. H.; Liu, G.; Lee, S.-Y.; Shea, K. J. Polymethylene-*block*-poly(dimethyl siloxane)-*block*-polymethylene Nanoaggregates in Toluene at Room Temperature. *Polymer* **2007**, *48*, 4123–4129.
25. Yin, L. G.; Hillmyer, M. A. Disklike Micelles in Water from Polyethylene-Containing Diblock Copolymers. *Macromolecules* **2011**, *44*, 3021–3028.
26. Schmalz, H.; Schmelz, J.; Drechsler, M.; Yuan, J.; Walther, A.; Schweimer, K.; Mihut, A. M. Thermo-Reversible Formation of Wormlike Micelles with a Microphase-Separated Corona from a Semicrystalline Triblock Terpolymer. *Macromolecules* **2008**, *41*, 3235–3242.
27. Ramzi, A.; Prager, M.; Richter, D.; Efstratiadis, V.; Hadjichristidis, N.; Young, R. N.; Allgaier, J. B. Influence of Polymer Architecture on the Formation of Micelles of Miktoarm Star Copolymers Polyethylene/Poly(ethylenepropylene) in the Selective Solvent Decane. *Macromolecules* **1997**, *30*, 7171–7182.
28. Xu, J.-T.; Jin, W.; Liang, G.-D.; Fan, Z.-Q. Crystallization and Coalescence of Block Copolymer Micelles in Semicrystalline Block Copolymer/Amorphous Homopolymer Blends. *Polymer* **2005**, *46*, 1709–1716.
29. Chan, S.-C.; Kuo, S.-W.; Lu, C.-H.; Lee, H.-F.; Chang, F.-C. Synthesis and Characterizations of the Multiple Morphologies Formed by the Self-Assembly of the Semicrystalline P4VP-*b*-PCL Diblock Copolymers. *Polymer* **2007**, *48*, 5059–5068.
30. Xu, J.-T.; Fairclough, J. P. A; Mai, S.-M.; Ryan, A. J. The Effect of Architecture on the Morphology and Crystallization of Oxyethylene/Oxybutylene Block Copolymers from Micelles in *n*-Hexane. *J. Mater. Chem.* **2003**, *13*, 2740–2748.
31. Walther, A.; Müller, A. H. E. Janus Particles. *Soft Matter* **2008**, *4*, 663–668.
32. Kretzschmar, I.; Song, J. H. Surface-Anisotropic Spherical Colloids in Geometric and Field Confinement. *Curr. Opin. Colloid Interface Sci.* **2011**, *16*, 84–95.
33. Walther, A.; Matussek, K.; Müller, A. H. E. Engineering Nanostructured Polymer Blends with Controlled Nanoparticle Location Using Janus Particles. *ACS Nano* **2008**, *2*, 1167–1178.
34. Jiang, S.; Chen, Q.; Tripathy, M.; Luijten, E.; Schweizer, K. S.; Granick, S. Janus Particle Synthesis and Assembly. *Adv. Mater.* **2010**, *22*, 1060–1071.
35. Wurm, F.; Kilbinger, A. F. M. Polymeric Janus Particles. *Angew. Chem., Int. Ed.* **2009**, *48*, 8412–8421.
36. Voets, I. K.; Fokkink, R.; Hellweg, T.; King, S. M.; de Waard, P.; de Keizer, A.; Cohen Stuart, M. A. Spontaneous Symmetry Breaking: Formation of Janus Micelles. *Soft Matter* **2009**, *5*, 999–1005.
37. Kuo, S.-W.; Tung, P.-H.; Lai, C.-L.; Jeong, K.-U.; Chang, F.-C. Supramolecular Micellization of Diblock Copolymer Mixtures Mediated by Hydrogen Bonding for the Observation of Separated Coil and Chain Aggregation in Common Solvents. *Macromol. Rapid Commun.* **2008**, *29*, 229–233.
38. McConnell, M. D.; Kraeutler, M. J.; Yang, S.; Composto, R. J. Patchy and Multiregion Janus Particles with Tunable Optical Properties. *Nano Lett.* **2010**, *10*, 603–609.
39. Du, J.; O'Reilly, R. K. Anisotropic Particles with Patchy, Multicompartment and Janus Architectures: Preparation and Application. *Chem. Soc. Rev.* **2011**, *40*, 2402–2416.
40. Glotzer, S. C.; Solomon, M. J. Anisotropy of Building Blocks and their Assembly into Complex Structures. *Nat. Mater.* **2007**, *6*, 557–562.
41. LoPresti, C.; Massignani, M.; Fernyhough, C.; Blanazs, A.; Ryan, A. J.; Madsen, J.; Warren, N. J.; Armes, S. P.; Lewis, A. L.; Chirasatitsin, S. Controlling Polymersome Surface Topology at the Nanoscale by Membrane Confined Polymer/Polymer Phase Separation. *ACS Nano* **2011**, *5*, 1775–1784.
42. Theodorakis, P. E.; Paul, W.; Binder, K. Interplay between Chain Collapse and Microphase Separation in Bottle-Brush Polymers with Two Types of Side Chains. *Macromolecules* **2010**, *43*, 5137–5148.
43. Njikang, G.; Han, D. H.; Wang, J.; Liu, G. J. ABC Triblock Copolymer Micelle-Like Aggregates in Selective Solvents for A and C. *Macromolecules* **2008**, *41*, 9727–9735.
44. Dupont, J.; Liu, G. J.; Niihara, K.; Kimoto, R.; Jinnai, H. Self-assembled ABC Triblock Copolymer Double and Triple Helices. *Angew. Chem., Int. Ed.* **2009**, *48*, 6144–6147.
45. Wunderlich, B. *Macromolecular Physics*; Academic Press: New York, 1976.
46. Nielsen, A. E. Nucleation and Growth of Crystals at High Supersaturation. *Kristall Technik* **1969**, *4*, 17–38.
47. Zhang, J. N.; Muthukumar, M. Monte Carlo Simulations of Single Crystals from Polymer Solutions. *J. Chem. Phys.* **2007**, *126*, 234904/1–234904/18.
48. Toda, A.; Kiho, H. Crystal Growth of Polyethylene from Dilute Solution: Growth Kinetics of {110} Twins and Diffusion-Limited Growth of Single Crystals. *J. Polym. Sci., Part B: Polym. Phys* **1989**, *27*, 53–70.
49. Flory, P. J. Thermodynamics of Crystallization in High Polymers. 4. A Theory of Crystalline States and Fusion in Polymers, Copolymers, and their Mixtures with Diluents. *J. Chem. Phys.* **1949**, *17*, 223–240.
50. Peterlin, A. Thickening of Polymer Single Crystals During Annealing. *J. Polym. Sci., Part B: Polym. Lett.* **1963**, *1*, 279–284.
51. Wunderlich, B.; Czornyj, G. A Study of Equilibrium Melting of Polyethylene. *Macromolecules* **1977**, *10*, 906–913.
52. Walther, A.; Barner-Kowollik, C.; Müller, A. H. E. Mixed, Multicompartment, or Janus Micelles? A Systematic Study of Thermoresponsive Bis-Hydrophilic Block Terpolymers. *Langmuir* **2010**, *26*, 12237–12246.

53. Kent, M. S.; Tirrell, M.; Lodge, T. P. Properties of Polystyrene-Poly(methyl methacrylate) Random and Diblock Copolymers in Dilute and Semidilute Solutions. *J. Polym. Sci., Part B: Polym. Phys.* **1994**, *32*, 1927–1941.
54. Richter, D.; Schneiders, D.; Monkenbusch, M.; Willner, L.; Fetters, L. J.; Huang, J. S.; Lin, M.; Mortensen, K.; Farago, B. Polymer Aggregates with Crystalline Cores: The System Polyethylene-Poly(ethylenepropylene). *Macromolecules* **1997**, *30*, 1053–1068.
55. Provencher, S. W. A Constrained Regularization Method for Inverting Data Represented by Linear Algebraic or Integral Equations. *Comput. Phys. Commun.* **1982**, *27*, 213–227.
56. Quintana, J. R.; Villacampa, M.; Katime, I. A. Micellization of a Polystyrene-*b*-poly(ethylene/propylene) Block Copolymer in *n*-Dodecane/1,4-Dioxane Mixtures. 2. Structure and Dimensions of Micelles. *Macromolecules* **1993**, *26*, 606–611.
57. Müller, A. J.; Balsamo, V.; Arnal, M. L. Nucleation and Crystallization in Diblock and Triblock Copolymers. *Adv. Polym. Sci.* **2005**, *190*, 1–63.
58. Lorenzo, A. T.; Arnal, M. L.; Müller, A. J.; de Fierro, A. B.; Abetz, V. Confinement Effects on the Crystallization and SSA Thermal Fractionation of the PE Block within PE-*b*-PS Diblock Copolymers. *Eur. Polym. J.* **2006**, *42*, 516–533.
59. Dupont, J.; Liu, G. J. ABC Triblock Copolymer Hamburger-Like Micelles, Segmented Cylinders, and Janus Particles. *Soft Matter* **2010**, *6*, 3654–3661.
60. Halperin, A. Polymeric vs. Monomeric Amphiphiles: Design Parameters. In *Supramolecular Polymers*; Ciferri, A., Ed.; Marcel Dekker, Inc.: New York, 2000.
61. Ruckdäschel, H.; Sandler, J. K. W.; Altstädt, V.; Rettig, C.; Schmalz, H.; Abetz, V.; Müller, A. H. E. Compatibilisation of Immiscible Blends by Triblock Terpolymers—Correlation between Block Copolymer Composition, Morphology and Properties. *Polymer* **2006**, *47*, 2772–2790.
62. Cotton, J. P. Initial Data Treatment. In *Neutron, X-Ray and Light Scattering*; Lindner, P., Zemb, T., Eds.; Elsevier Science Publishers B. V.: Amsterdam, 1991.
63. Brulet, A.; Lairez, D.; Lapp, A.; Cotton, J.-P. Improvement of Data Treatment in Small-Angle Neutron Scattering. *J. Appl. Crystallogr.* **2007**, *40*, 165–177.
64. Kohlbrecher, J. *SASfit: A Program for Fitting Simple Structural Models to Small Angle Scattering Data*; Paul Scherrer Institute, Laboratory for Neutron Scattering: CH-5232, Villigen Switzerland, 2008.